DEUTSCHES ELEKTRONEN-SYNCHROTRON DESY

DESY 80/100
October 1980

THE TASSO GAS AND AEROGEL CERENKOV COUNTERS

by

H. Burkhardt, P. Koehler, R. Riethmüller, B. H. Wiik
Deutsches Elektronen-Synchrotron DESY, Hamburg

R. Fohrmann, J. Franzke, H. L. Krasemann, R. Maschuw, G. Poelz,
J. Reichardt, J. Ringel, O. Römer, R. Rüsch, P. Schmüser, R. van Staa
II. Institut für Experimentalphysik der Universität Hamburg

J. Freeman, P. Lecomte, T. Meyer, Sau Lan Wu, G. Zobernig
University of Wisconsin, Madison, Wisconsin, USA

NOTKESTRASSE 85 · 2 HAMBURG 52

To be sure that your preprints are promptly included in the HIGH ENERGY PHYSICS INDEX , send them to the following address (if possible by air mail) :

DESY
Bibliothek
Notkestrasse 85
2 Hamburg 52
Germany

DESY 80/100
October 1980

THE TASSO GAS AND AEROGEL CERENKOV COUNTERS

H.Burkhardt, P.Koehler*, R.Riethmüller, B.H.Wiik,

Deutsches Elektronen-Synchrotron DESY, Hamburg, Germany

R.Fohrmann, J.Franzke, H.L.Krasemann, R.Maschuw**, G.Poelz, J.Reichardt, J.Ringel***, O.Römer, R.Rüsch, P.Schmüser, R. van Staa,

II. Institut für Experimentalphysik+, Universität Hamburg, Germany

J.Freeman, P.Lecomte, T.Meyer, Sau Lan Wu, G.Zobernig,

University of Wisconsin++, Madison, Wisconsin, USA

Submitted to Nuclear Instruments and Methods.

* On leave from FNAL, Batavia, Illinois, USA
** Now at Kernforschungszentrum Karlsruhe, Germany
*** Now at CERN, Geneva, Switzerland

+ Supported by the Deutsches Bundesministerium für Forschung und Technologie
++ Supported in part by the US department of Energy, Contract WY-76-C-02-0881

Abstract:

We describe the gas and aerogel threshold Cerenkov counters built for the TASSO experiment at the DESY e^+e^- storage ring PETRA. The counters are arranged in two diametrically opposed groups as part of the two hadron arms. The gas counters contain Freon 114 and CO_2 respectively; 128 ellipsoidal mirrors focus the Cerenkov light through funnels onto Philips 5" photomultipliers coated with wavelength shifter. $\beta = 1$ charged particles are detected with at least 99.9% efficiency. The aerogel counters are of the diffusing wall type. They have a sensitive area of 12 m^2, divided into 32 cells and use a total of 192 RCA Quantacon 5" photomultipliers. The average aerogel refractive index is around 1.025. The efficiency for $\beta = 1$ charged particles is 98%. Design considerations, prototype evaluation, construction details, and performance of the final counter system are described.

1. Introduction

The Two Arm Spectrometer Solenoid TASSO (Fig. 1) is a large experimental setup designed to study e^+e^- interactions at the DESY storage ring PETRA. Its main part is a central detector[1)] with a 0.5 tesla axial magnetic field and 19 concentric layers of proportional and drift chambers for track reconstruction and momentum measurement as well as 48 time-of-flight counters for triggering and low momentum particle identification. A unique feature of TASSO is the presence of two hadron arms, providing almost complete particle identification over 20% of 4π steradian. Each hadron arm consists of a single layer drift chamber with correlated two-dimensional readout, 16 sets of aerogel, Freon 114 and CO_2 Cerenkov counters, time-of-flight scintillators, lead-scintillator shower counters, and proportional tubes behind 87 cm of iron for muon identification.

The hadron arms are installed symmetrically with respect to the colliding beams to allow the study of correlations in back-to-back jets. Although the full particle identification capabilities of the system depend on all of the components listed above, we will limit ourselves here to a description of the Cerenkov counters.

The counters are subdivided into 16 mechanically separated cells per arm, each covering a range of about 10^{o} in the production angle θ and 26^{o} in the azimuthal angle ϕ. Each gas cell is subdivided by two mirrors collecting the light onto different phototubes. The main motivation for the fine granularity was to avoid that several tracks of a hadronic jet enter the same Cerenkov cell and confuse the particle identification. The choice of refractive indices resulted from the following considerations: owing to the size of the system, and for safety reasons, it was judged impractical to build pressurized counters or to use inflammable gases. The highest refractive index at atmospheric pressure is then provided by Freon 114 ($C_2Cl_2F_4$, $n = 1.0014$), permitting pion identification above 2.7 GeV/c. Such counters combined with others using CO_2 ($n = 1.00043$) and a medium with $n = 1.016$ respectively will give full pion identification over the whole momentum range and kaon identification everywhere except between 5.5 and 9.5 GeV/c, where there is an ambiguity with protons.

A refractive index of $n = 1.016$ can be achieved with silica aerogel, but the light output appeared somewhat marginal. It was therefore decided to take $n = 1.025$ and to accept a gap in kaon identification. The threshold momenta for pions, kaons, and protons are summarized in Table 1.

2. The gas threshold Cerenkov counters

2.1 Design of the gas counters

The optical system of the gas counters has been specifically layed out for the application at an e^+e^- storage ring where the center-of-mass system is identical to the laboratory system and secondary particles emerge from a small region around the well defined interaction point. The Cerenkov light generated by a charged particle follows the particle track and, in the absence of a magnetic field, it appears to a good approximation to come from the interaction point. In that case, optimum focusing is achieved by concave ellipsoidal mirrors having one focal point at the interaction vertex and the other at the corresponding phototube (see Fig. 2). Such a counter concept has been successfully applied by our group in the DASP detector[2] at DORIS and by the DELCO collaboration[3] at SPEAR.

The light collection has been simulated with a Monte Carlo program, taking into account the size of the interaction region, the Cerenkov angle, the deflection of the particle trajectory in the magnetic field, the reflectivity of the mirrors, and the optical properties of the radiator. In the TASSO counters, the Cerenkov light is imaged in the focal plane of the mirrors into a ring of up to 20 cm in diameter, depending on the gas and the particle velocity. For a particle momentum of 2.7 GeV/c, corresponding to the pion threshold in Freon 114, the center of the ring is shifted by about 3 cm because of the deflection of the particle in the magnetic field. For these reasons, light funnels of the Winston type[4] are used to collect the light onto the 5" photomultipliers. The computed photon distributions at the entrance of the funnel and on the photocathode (Fig. 3) for $\beta = 1$ particles and for pions of 3 GeV/c, show that the light of a cell can indeed be focused on a single 5" tube. The length and diameter of the light funnels were also optimized with the Monte Carlo simulation and by accepting some compromise we were able to build the entire system with only two sizes of funnels.

2.2 Fabrication of the ellipsoidal mirrors

It can be seen from Fig. 1 that there are four types of almost identical Cerenkov cells at slightly different distances from the interaction point. To facilitate mirror production the parameters of the ellipsoids were standardized. The focusing properties are sufficiently good for all cells. The half axes of the four ellipsoids and the mirror sizes are listed in Table 2.

The mirrors were made of 2 mm thick heat-formed lucite sheets, aluminized on the front surface and backed by a light and rigid sandwich structure (Fig. 4). A negative aluminum mold was made for each of the four mirror types. The first mold was carved out of a massive aluminum plate with a numerically-controlled milling machine[5] but casting proved to be less expensive. The other three molds were first built as wooden models[6], using computer-plotted templates, and then cast in aluminum. The casts needed some manual grinding to correct for shrinkage (up to a few mm). All molds were polished by hand. They were then used as mother molds to heat-form 2 mm thick lucite sheets[7]. The formed lucite sheets were cut to their final size with a fine band saw and

thoroughly cleaned. The aluminization was done at DESY. A vacuum of better than 10^{-5} mbar and a short evaporation time of 20 sec were found to be essential for high reflectivity and long term stability. We took advantage of a getter pumping effect by first evaporating some aluminum away from the mirror. Six to eight tungsten coils wrapped with aluminum wire of 99.99% purity were heated simultaneously to produce a uniform aluminum layer of 60 to 80 nm thickness. The reflectivity was measured for wavelengths between 230 and 600 nm and found to be around 90%, close to the theoretical limit for aluminum. The reflective layer was not coated with magnesium fluoride because the natural oxydation of the aluminum proved to provide sufficient protection even after several months of storage in dry air.

The 2 mm thick lucite mirrors were extremely flexible and had to be reinforced by a rigid backing. A sandwich structure was chosen because of its low weight and good mechanical properties. The core material is 19 mm thick Nomex polyamide honeycomb with a cell size of 5 mm and a density of 29 kg/m^3 (Aeroweb A1, Ciba-Geigy). The honeycomb was sandwiched between thin epoxy-fiberglass layers on positive molds which were obtained as epoxy-fiberglass replicas of the original aluminum molds. After a curing time of 12 hours at 40^o C the backings became very rigid and kept their shape to within a few tenths of a mm. They have a weight of only 0.21 g/cm^2 and are thus lighter than the lucite mirrors (0.24 g/cm^2).

The aluminized mirrors were glued to the backings with age-resistant double-sticky tape (Tesafix 950, BDF Corporation) having a 0.8 mm polyurethane foam core to allow for slight mismatching between mirror and backing.

2.3 Light funnels and photomultipliers

The Winston type light collectors in front of the phototubes increase the effective cathode area. Their shape is obtained by rotating a parabola around an axis making an angle α with the symmetry axis. This angle α is then the acceptance angle of the resulting funnel. Light rays with an angular divergence smaller than α are collected onto the photocathode. Two sizes of light funnels are used: type W 1 has an entrance diameter of 31 cm and an acceptance angle $\alpha = 19.5^o$, type W 2 has a diameter of 23 cm and $\alpha = 26^o$.

The funnels were fabricated by expanding preheated lucite tubes into an aluminum mold using compressed air[8]. The aluminization was done at DESY using two tungsten coils and rotating the funnel during evaporation. The gas Cerenkov counters use 5" phototubes Philips XP 2041 mounted within the gas volume. These tubes have a bialkali photocathode and a glass envelope with reasonably good ultraviolet transparency. To improve the UV response, the cathode was coated with a wavelength shifter[9], merely by dipping the tube window in a solution of p-terphenyl and polystyrol in methylenchloride. This increased the overall photoelectron yield by about 30%, as measured with an air filled Cerenkov counter.

The magnetic shields consist of outer steel and inner mumetal cylinders with a large entrance diameter to accommodate the light funnels. The transverse component of the TASSO magnet fringe field is well shielded but the longitudinal component at the position of the Freon counters is of the order of one gauss inside the shielding and decreases the photoelectron collection in the tube by up to a factor of 2. This component is compensated by a 350 turns bucking coil wound around the inner mumetal cylinder and requiring about 50 mA. The inner mumetal cylinder is at cathode potential to avoid leakage currents.

2.4 Construction of the cells

The design of the mechanical structure was guided by the following considerations: with a minimum amount of material along the particle path a very rigid support for the optics as well as for the phototube shieldings had to be provided. At the same time the structure had to be gas tight, reasonably lightweight, and transportable. The solution adopted was to divide one hadron arm into four modules, each module consisting of four complete sets of Cerenkov counters. The modules were built with sandwich plates of aluminum honeycomb and epoxy-fiberglass material, (Aeroweb F Board, Ciba-Geigy, 3.1 kg/m^2 for 13 mm thickness). The plates were assembled with polyurethane glue and reinforced near the phototubes with aluminum frames to permit mounting of the aluminum boxes which house the phototube shields (Fig. 2). Gas and light tightness of the cells were achieved by several layers of black polyurethane paint. The assembled four-cell modules

are very sturdy and can easily support the weight of the phototube shields (800 kg for 40 tubes). Within each cell, the aerogel, Freon, and CO_2 counters are arranged sequentially and separated by gas tight windows made from 1 mm clear polycarbonate sheets (Makrolon, Bayer Leverkusen).

The mirrors were installed from below. For this reason, the top modules had to be turned upside down. The structure proved to be rigid enough so that mirror alignment was not affected by the rotation. The mirrors were aligned by means of a light source at the nominal interaction point. After the alignment the windows were covered with black foil. The bottom modules are mounted on a movable platform and are sufficiently rigid to support the top modules directly. The overall Cerenkov system of one hadron arm is about 7 m wide, 7 m high and 3.3 m deep but weighs less than 8 tons including magnetic shieldings.

2.5 Performance of the gas counters

A full scale prototype was tested in a pion beam at CERN. The threshold curve measured with Freon 114 is shown in Fig. 5. The efficiency rises steeply above 2.7 GeV/c and reaches a plateau value of 99.9% with a systematic error of about 0.2% due to background.

Assuming Poisson statistics for the emission of photoelectrons from the photomultiplier cathode the efficiency ε of the counter is related to the average number of photoelectrons $\langle N_e \rangle$ by

$$\varepsilon = 1 - \exp(-\langle N_e \rangle).$$

Here we have assumed that the gain of the phototube is sufficiently high that single photoelectrons are detected with good efficiency.

It is customary to parametrize $\langle N_e \rangle$ as $\langle N_e \rangle = N_0 \, L \sin^2\theta_c$ where θ_c is the Cerenkov angle, and L the length of the radiator. N_0 is a "quality factor" which is the integral of the $1/\lambda^2$ Cerenkov spectrum, folded with the

quantum efficiency of the photomultiplier*, the reflectivity of the mirrors, and the optical transmission of Cerenkov radiator and phototube windows.

The wavelength dependence of these quantities is plotted in Fig. 6. It can be seen that the application of a wavelength shifter improves the UV response of the phototubes considerably. Freon 114 shows strong absorption below 220 nm, whereas in the CO_2 counters the mirrors and phototubes are also limiting factors. Performing the integration [23] we predict $N_0 = 110\ cm^{-1}$ for the Freon counters and $N_0 = 150\ cm^{-1}$ for the CO_2 counters, with a systematic uncertainty of about 25%.

The factor N_0 has also been determined experimentally: using the Cerenkov relation

$$\cos\theta_c = 1/n\beta$$

one obtains

$$N_e = N_0 \cdot L \cdot (1 - 1/n^2\beta^2)$$

hence the number of photoelectrons in the threshold region should depend linearly on $1/\beta^2$. This is indeed found to be the case (cf. Fig. 8c where such a plot is shown for the aerogel counters). Extrapolating the straight line to $1/\beta^2 = 1$ we obtained $N_0 = 90\ cm^{-1}$ for the Freon counter (we have not measured N_0 for the CO_2 counter because the pion momentum in the test beam was limited to 4 GeV/c). This means that $\beta = 1$ particles produce about 20 photoelectrons in Freon 114 and, as a conservative estimate, at least 8 in CO_2, leading to negligible inefficiencies.

A scan across the counter area was made to check for possible inefficiencies close to the walls and at the boundary between the two mirrors in a cell. For $\beta = 1$ particles the efficiency was found to be safely above 99% outside a margin of 1 cm along the rim of the mirrors.

---

* The quantum efficiency, as measured in a short air filled Cerenkov counter, appears lower than the value given by the manufacturer of the tubes. This problem has been reported earlier [10] and has been attributed to a photoelectron collection efficiency of 60% between photocathode and first dynode.

The final counter system was tested with cosmic ray muons recorded in parallel to normal data taking runs at PETRA. Only the counters below the mid-plane of the TASSO detector could be tested because in the top counters the cosmic rays travel in the wrong direction. The tracks and momenta of the muons were reconstructed using the central detector. The statistics is fairly limited since the focusing optics requires the cosmic rays to pass through a small volume around the nominal interaction point. The efficiency for high momentum muons, averaged over all bottom cells, was measured to be $(99 \pm 1)\%$ in both the Freon and CO_2 counters (statistical errors only).

3. Aerogel Cerenkov counters

3.1 Properties of aerogel

The use of silica aerogel as a Cerenkov radiator has been studied in Ref. 11 to 13. Silica aerogel is a very light silicon dioxide structure containing a large number of microscopic pores with diameter smaller than the wavelength of the light[14,15]. The effective index of refraction is given as an average over the SiO_2 and the enclosed air, typical values being $n = 1.02$ for a density of 0.1 g/cm^3.

We have made an extensive study of the various parameters affecting the aerogel quality and a summary of our work can be found elsewhere[16,17]. The production of aerogel is a complex and lengthy process and will be sketched only briefly here. A detailed description of the procedure followed in our laboratory at DESY will appear in a separate publication.

In a first step, an alcogel is formed by polymerization of orthosilicic acid in methanol; the pores of this gel are filled with the solvent. About one week of aging time is needed after gelification. To remove the liquid without damaging the gel structure one must heat the mixture above the critical point of the alcohol; for this purpose the alcogel is slowly heated up to 270^0 C at a pressure of 120 bars within a period of 24 hours and then the alcohol is extracted. The resulting aerogel pieces are already useful for Cerenkov counters but their optical transparency can be further improved

by baking them for 3 hours at 400^{0}C in air at atmospheric pressure to remove organic residues.

In our laboratory the aerogel is produced in pieces of 17 x 17 x 2.3 cm^3 at a rate of 100 to 150 pieces a week. For each piece the index of refraction and the transparency are measured; indices from 1.020 to 1.026 and scattering lengths of more than 2 cm (at λ = 436 nm) were accepted for the TASSO counters. The production yield improved from 30% initially to 90% in recent months; rejects are mainly due to cracks or insufficient transparency.

The optical properties of aerogel can be characterized by an absorption length l_a and a scattering length l_s both of which are strongly wavelength dependent. In the visible region, the absorption length is usually much larger than the scattering length hence most of the light removed from a well collimated light beam is actually not absorbed but rather scattered out of the direct path. A measurement of the scattering length is therefore straightforward. The average value for our aerogel production is l_s = 2.4 cm at λ = 436 nm; l_s varies with the wavelength $\propto \lambda^{-4}$ since the diffusion of the light is caused by Rayleigh scattering on the microscopic pores. The absorption length can only be determined indirectly, e.g. by measuring the decay time of a short light pulse inside a highly reflective box containing a sample of aerogel, and comparing the result to a Monte Carlo simulation. Above 300 nm we find values for l_a which are 10 to 100 times larger than l_s. But as the absorption length decreases strongly in the near ultraviolet our aerogel does not yield significant amounts of Cerenkov light below 300 nm.

3.2 Light collection in the aerogel counters

Two basically different techniques of light collection have been considered: A system with focusing mirrors similar to that of the gas counters, and a diffusing wall type system where the photons undergo several diffuse scatterings on highly reflective white walls before reaching a phototube. A focusing optics can of course collect only the direct (unscattered) Cerenkov light and is therefore restricted to small aerogel thickness. In the diffusing wall system both direct and diffusely scattered photons have a chance to be detected; the lower collection efficiency can be compensated by increasing the aerogel thickness.

To decide between the two possibilities, measurements with small imaging and diffusing test counters were performed in a DESY test beam. In the first test, cylindrical aerogel samples were placed in a black tube which absorbed most of the scattered light. The direct light was collected via a mirror onto a 5" quantacon photomultiplier (RCA 8854). The number of photoelectrons is plotted in Fig. 7a as a function of the aerogel thickness d for three refractive indices. The curves saturate at about 8 cm and can be parametrized as

$$N_e(x) = N_e(\infty)\ (1 - \exp(-x/l_s))$$

with $l_s = 1.7 \pm 0.1$ cm and $x = d/\cos\theta_c$. From this measurement it was concluded that for $n = 1.025$ about 7 photoelectrons could be obtained with a perfect optical system.

In the second test a small box was lined with Millipore paper[18] with a reflectivity of more than 95% above $\lambda = 400$ nm. A single RCA 8854 phototube served to detect the Cerenkov light generated in an aerogel stack of up to 18 cm thickness. The number of photoelectrons shows a steady, though not linear, increase with thickness and reaches a value of 12 (Fig. 7b), indicating that a diffusing type counter might be a promising approach for the TASSO system*.

Light collection in the TASSO aerogel cells is a much more difficult task than in the small test counters; the light from a large aerogel area (35×100 cm^2) has to be collected onto phototubes outside the geometric acceptance of the counter (Fig. 2).

Both focusing and diffusing type counters were studied in Monte Carlo simulations. The large Cerenkov angle (12.7^o for $n = 1.025$) prohibits focusing on a single 5" phototube 1 - 2 m away from the aerogel, but even the most elaborate focusing system, using 6 tubes per cell with Winston cones and elliptical mirrors, could at best achieve an average light collection

* It should be noted that in both tests counters unbaked aerogel was used and that the aerogel in the final TASSO counters has about 30% more light output due to improved transparency.

efficiency of 50% corresponding to 3.5 photoelectrons, however varying from 30 to 60% across the counter area. From this we concluded that a focusing aerogel counter using only direct light was just marginally feasible for the TASSO geometry; moreover, the complexity of the optical system appeared incompatible with the time schedule of the experiment.

The light collection efficiency of a large diffusing box is lower than what can be obtained with a focusing system but diffused light as well as direct light is collected, so that the usable aerogel thickness is not anymore limited by the scattering length but rather by the considerably longer absorption length. Compared to a focusing system this approach requires about 3 times more aerogel, demands diffusing walls with high reflectivity (> 95%) and has a larger time spread (a gate of 200 ns is necessary) but the construction is simpler, aerogel quality is less critical and satisfactory uniformity of the light collection can be obtained. The light collection efficiency is roughly proportional to the ratio of photocathode to wall area, implying in practice that several large diameter tubes with high quantum efficiency are necessary in a large aerogel cell. For a configuration of six RCA 8854 quantacon tubes per cell and 20 cm of aerogel the Monte Carlo simulation predicted an average of about 4 photoelectrons with good uniformity over the counter area.

Tubes with large cathodes like the Philips 60 DVP were considered but rejected since it seemed difficult to protect them against the 20 - 50 gauss fringe field of the TASSO magnet. The presence of this field also degrades the light collection efficiency with 5" photomultipliers because the tubes have to be recessed by 14 cm into the shields, and light funnels must be added.

A full scale prototype cell with six RCA 8854 phototubes was built. The walls were lined with millipore fixed to white cardboard with double-sticky tape. The millipore covered an area of 40000 cm^2 whereas the aerogel and photocathode areas were 3400 cm^2 and 600 cm^2 respectively. An estimate of the light collection efficiency is given by the expression[19]:

$$\eta = t \cdot f / (1-(1-f)R)$$

where f = 0.014 is the fraction of photocathode area, R = 0.92 is the reflectivity of the walls taken as a weighted average over the millipore and aerogel, and t = 0.8 is the estimated transmission of the light funnels. This gives $n = 0.12$ for the prototype cell.

For small values of f the collection efficiency is directly proportional to the total photocathode area; moreover it is critically dependent on the millipore reflectivity: changing it from 95 to 94% reduces n from 0.12 to 0.11.

The prototype was tested in pion beams at DESY and CERN. The threshold curve obtained for 18 cm of unbaked aerogel with $n = 1.024$ is plotted in Fig. 8a. A steep rise at a pion momentum of 0.65 GeV/c is observed, followed by a plateau region with an efficiency of 98% for $\beta \to 1$, corresponding to 3.9 photoelectrons.

The number of photoelectrons in the plateau, measured as a function of the aerogel thickness d, is shown in Fig. 8b. The data are well represented by the form

$$\langle N_e \rangle \propto (1 - \exp(-d/\Lambda_a))$$

Here Λ_a is an effective absorption length, which takes into account the photon path resulting from diffuse scattering.

A fit to the data yields $\Lambda_a = 9 \pm 1$ cm. Thus a slab of aerogel of thickness d, used in a diffusing counter, has an effective thickness

$$d_{eff} = \Lambda_a (1 - \exp(-d/\Lambda_a)).$$

In analogy with gas counters, the number of photoelectrons is given by

$$\langle N_e \rangle = N_0 d_{eff} \sin^2\theta_c = N_0 d_{eff}(1-1/n^2\beta^2) = n_0 n d_{eff} (1-1/n^2\beta^2)$$

Fig. 8 c demonstrates this linear dependence. Extrapolating to $1/\beta^2 = 1$, we obtained $N_0 = 10.7 \pm 0.1$. If we divide this by the estimated light collection efficiency $n = 0.12$, we get $n_0 = 90\ cm^{-1}$. This can be compared with $n_0 = 110\ cm^{-1}$ for the Freon counter, which has a light collection efficiency of 80%.

From the slope of the straight line, the index of refraction can be computed: the result is $n = 1.024 \pm 0.001$ in agreement with the optical measurement.

The data in Fig. 8a show a detection efficiency of (6 ± 2)% at 0.4 GeV/c, below muon threshold. Most of this is due to knock-on electrons produced in the material upstream and in the aerogel itself, each contributing about 2% according to a Monte Carlo study. The amount of light produced in the millipore was measured in the prototype counter with 3.4 GeV/c pions: we inserted several adequately spaced layers of millipore into the particle path and found a light yield of about 1.2×10^{-2} photoelectron/layer, linearly dependent on the number of layers.

3.3 Phototubes and associated electronics

Two types of 5" bialkali phototubes have been considered, the Philips XP 2041 and the RCA 8854. Both tubes have similar quantum efficiencies and spectral responses, but as we operate each tube essentially at the single photoelectron level, the 8854 quantacon proved to be superior, owing to its better single photoelectron spectrum. The noise spectrum of the quantacon tube shows a single photoelectron peak well separated from other sources of noise; this peak is very useful for adjusting the absolute gain of the tubes and defining the electronics threshold (by a software cut on the pulse height spectrum). The XP 2041 was ruled out since it has a quasi-exponential noise spectrum and low thresholds, combined with extremely stable operating conditions, are needed to detect single photoelectrons consistently with good efficiency. This is a well-known problem[20] attributed to the inhomogeneity and low gain of the first dynode of the XP 2041.

The voltage distribution used with the quantacon is linear; the maximum permitted voltage of 1000 volts is applied between cathode and first dynode for improved electron collection efficiency. Six tubes were tested up to 1600 Volts without further improvements. Each tube is connected to its own ADC (LeCroy 2282A). The high voltage is adjusted to produce a gain of 2.5×10^8. Each cell is illuminated by an LED which serves two purposes: first to check and calibrate the phototubes, and second to monitor the re-

flectivity of the walls by measuring the characteristic decay time of the light within the cell. In counters with diffusing walls, photons can bounce around for a relatively long time before being absorbed or reaching a phototube; the longer this time, the better the reflectivity of the walls. The intensity of a short light pulse is observed to decrease exponentially in our counters with a time constant of 45 to 50 ns for green light.

3.4 Description and performance of the final system

The aerogel cells were lined with millipore in a dust-free environment. Each of the 32 cells has an entrance window of about 35 x 100 cm^2. Due to limited production rate an aerogel thickness of 13.5 cm was chosen although the test measurements had shown that 18 to 20 cm would be optimal. The resulting light loss is essentially compensated by the improved optical quality of the more recently produced aerogel. The refractive index ranges from 1.023 to 1.026 except in eight cells which have values between 1.020 and 1.023. The aerogel pieces were cut to their accurate size with a diamond saw and then stacked in the cells; they are held in place by cotton strings.

The detection efficiency of the final counter system was measured with cosmic ray muons recorded in parallel to normal data taking runs at PETRA. Again, this can be done reliably only for the counters below the mid-plane of the detector*. The efficiency, averaged over all bottom cells and a running period of 2 months, is plotted in Fig. 9 as a function of muon momentum.

Using the ADC information and the threshold behaviour, we deduce a mean number of photoelectrons for $\beta \to 1$ particles:

$$\langle N_e \rangle = 3.9 \pm 0.2 \ .$$

* The amount of light measured in the top cells is about 70% of that in the bottom cells which means that most photons lose the information on the track direction.

4. Summary and Conclusion

We have built and successfully operated a large system of aerogel and gas Cerenkov counters making use of low refractive index aerogel in a difficult geometry. The combination of atmospheric pressure gas counters and aerogel is providing particle identification over a wide momentum range with acceptable segmentation and solid angle coverage at PETRA energies. The problems of manufacturing large amounts of aerogel of good optical properties with excellent production yields have been solved for refractive indices $n \geq 1.020$ (good samples have been obtained for n as low as 1.007). The system as it stands promises to be a useful tool for physics at PETRA and a source of experience for the design of similar equipment in anticipation of experiments at LEP and HERA. First results on pion, kaon and proton separation in hadronic final states from e^+e^- annihilation have been presented at the 1980 Wisconsin conference on high energy physics[21]. In view of the higher than expected multiplicity at PETRA[22] and the marked jet structure, it was particularly interesting to measure the percentage of cases in which more than one track goes into a given aerogel cell. It varies from 15% at a center of mass energy of 13 GeV to 25% at 36 GeV. The gas Cerenkov counters have twice as much segmentation in ϕ, therefore the percentage of ambiguity is correspondingly lower: 6% at 13 GeV and 15% at 36 GeV.

Acknowledgements

We want to thank all the people who contributed to the design, construction and test of the Cerenkov counters. We are particularly indebted to the technical staffs of DESY and of the II. Institut of the University of Hamburg for their constant help, namely to H.Arndt, U.Balszuweit, H.Bock, G.Bömelburg, D.Brauer, J.Dicke, E.Dinges, W.Heller, G.Krohn, R.Landrock, B.Lücke, H.-J. Schirrmacher, C.-H.Sellmer and T.Stötzer. Particular thanks are due to M.Holder and H.L.Lynch for their assistance during the prototype evaluation as well as to J.Weber and his workshop staff for their continuous support.
We gratefully acknowledge the support received from the CERN management and the technical staff of the South Hall during the tests performed at the PS, and thank Mr. R.Schillsott for the invaluable help he provided. One of us (P.K.) would like to thank the Alexander von Humboldt Foundation for support through a Humboldt award.

Table 1 - Refractive indices and threshold momenta of the TASSO Cerenkov counters

radiating medium	refractive index	thresholds (GeV/c) Pion	Kaon	Proton
Aerogel	1.025	0.6	2.2	4.2
Freon 114	1.0014	2.7	9.4	17.8
CO_2	1.00043	4.8	16.9	32.0

Table 2 - Parameters of the optics for the TASSO gas Cerenkov counters (see also Figure 2)

mirror type	x and y half-axes (mm)	z half-axis (mm)	approximate dimensions (mm^2)
B 1	1868	2626	1050 x 650
B 2	2334	2887	1090 x 690
C 1	2324	3486	1380 x 800
C 2	2788	3621	1360 x 885

light funnel type	acceptance angle	entrance radius (mm)	exit radius (mm)	length (mm)
W 1	19.5^0	154	52.5	450
W 2	26.0^0	116	52.5	250

References:

1) Properties of hadron final states in e^+e^- annihilation at 13 GeV and 17 GeV center of mass energies
TASSO Collaboration, Phys.Lett. 83B, 261 (1979)

The large cylindrical drift chamber of TASSO
H.Boerner et al., DESY 80/27 - to be published in Nucl.Instr.Meth.

2) Evidence for weakly decaying new hadrons in e^+e^- collisions above 4 GeV cms
DASP Collaboration, Phys.Lett. 63B, 471 (1976)

3) A large solid angle Cerenkov counter for the DELCO experiment at SPEAR
W.E.Slater et al., Nucl.Instr.Meth. 154, 223 (1978)

4) Efficient light coupler for threshold Cerenkov counters
H.Hinterberger, R.Winston, Rev.Sci.Instr. 37, 1094 (1966)

5) Machining was done by MBB Hamburger Flugzeugbau.

6) The wooden models and the aluminum casts were made by Wendt Modellbau, Neu Wulmstorf.

7) The heat-forming of the mirrors was done by the companies Kopperschmidt and Nordform, Hamburg, using high planarity plexiglas protected by a non-adhesive polyethylene foil.

8) The Winston funnels were fabricated by Nordform, Hamburg. The shape of the mold had been corrected for the change in lucite thickness during the heat-forming and for the lucite shrinkage during cooling.

9) Method for elimination of quartz-face phototubes in Cerenkov counters by use of wavelength shifter
E.L.Garwin et al., Nucl.Instr.Meth. 107, 365 (1973)

A method of coating photomultipliers with wavelength shifters
G.Eigen and E.Lorenz, Nucl.Instr.Meth. 166, 165 (1979)

10) The use of photomultiplier tubes for photon counting
R.Foord et al., Applied Optics 8, 197 (1969)

Ultraviolet Cerenkov light detector
P.Baillon et al., Nucl.Instr.Meth. 126, 13 (1975)

11) Silica Aerogels used as Cerenkov radiators
M.Cantin et al., Nucl.Instr.Meth. 118, 177 (1974)

12) Use of Silica Aerogel for Cerenkov Radiation Counter.
M.Bourdinaud et al., Nucl.Instr.Meth. 136, 99 (1976)

13) Test of large Cerenkov detectors with Silica Aerogel as radiator
M.Benot et al., Nucl.Instr.Meth. 154, 253 (1978)

14) The colloid chemistry of Silica and Silicates
R.K.Iler, Cornell University Press, New York 1955

15) C.Okkerse in "Physical and chemical aspects of adsorbents and catalysts", B.G.Linsen editor. Academic press London and New York 1970, p. 213

16) Herstellung und Test von Siliziumdioxyd Aerogel für den Einsatz in Cerenkovzählern
N.Kuschnerus - DESY F 35 - 78/01

17) Untersuchungen zur Herstellung von Aerogel für die TASSO Cerenkov-Zähler
R.Riethmüller - DESY F 35 - 79/01

18) Millipore paper type GS available from Millipore Company Corp. Bedford, Mass. (USA)

19) Technique for painting light integrating boxes
S.P.Ahlen et al., Nucl.Instr.Meth. 143, 513 (1977)

20) Photomultipliers - Philips Application book (p. 76)

21) Features of inclusive hadron production in e^+e^- annihilation at PETRA
D.Pandoulas, 14th International Conference on High Energy Physics, Madison, Wisconsin (1980)

22) Rapid growth of charged particle multiplicity in high energy e^+e^- annihilations, TASSO Collaboration, Phys.Lett. 89B, 418 (1980)

23) Gas-Cerenkovzähler für TASSO - H.Burkhardt - DESY F 35 - 80/01

Figure Captions:

Fig. 1 Top and end views of the TASSO detector showing the central detector and the hadron arms.

Fig. 2 View of one Cerenkov unit, showing the Aerogel, Freon 114 and CO_2 counters. The optics of the gas counters is the same for all cells, despite different distances to the interaction point. Light collection is shown schematically.

Fig. 3 Computed distribution of the light at the entrance of the funnel and on the phototube for $\beta = 1$ particles (a,b), and for 3 GeV/c pions (c,d). The Monte Carlo simulation includes the effect of the magnetic field.

Fig. 4 Detail of the mirror: the 2 mm thick aluminized lucite is glued with double-sticky tape onto an epoxy-fiberglass and Nomex honeycomb sandwich. The overexpanded type of honeycomb is used rather than the conventional hexagonal one since it follows the bidimensional curvature of the mirror molds much more easily.

Fig. 5 Threshold curve of the Freon 114 prototype counter measured in a pion beam. The plateau corresponds to 99.9% efficiency with a 0.2% systematic error.

Fig. 6 Wavelength dependence of the quantities characterizing our gas Cerenkov counters:
Cerenkov light intensity $I(\lambda) = 2\pi\alpha/\lambda^2$, plotted in arbitrary units; reflectivity of our mirrors, transparency of 1 m CO_2 and of Freon 114 at NTP (left hand scale); quantum efficiency of the XP 2041 photomultiplier with and without wavelength shifter (right hand scale).

Fig. 7a Number of photoelectrons vs. aerogel thickness in an imaging test counter which measures only direct (unscattered) Cerenkov light.

Fig. 7b Number of photoelectrons vs. aerogel thickness in a small diffusing counter with highly reflective white walls (millipore, reflectivity > 95% above λ = 400 nm).

Fig. 8 a) Threshold curve of the prototype aerogel counter in a pion beam. Aerogel thickness 18.5 cm.

b) Average number of photoelectrons vs. aerogel thickness in the prototype counter for 3.4 GeV/c pions.

c) The average number of photoelectrons plotted against $1/\beta^2$.

Fig. 9 Threshold curve with cosmic ray muons for the final TASSO aerogel counters. Plotted is the average over all bottom cells.

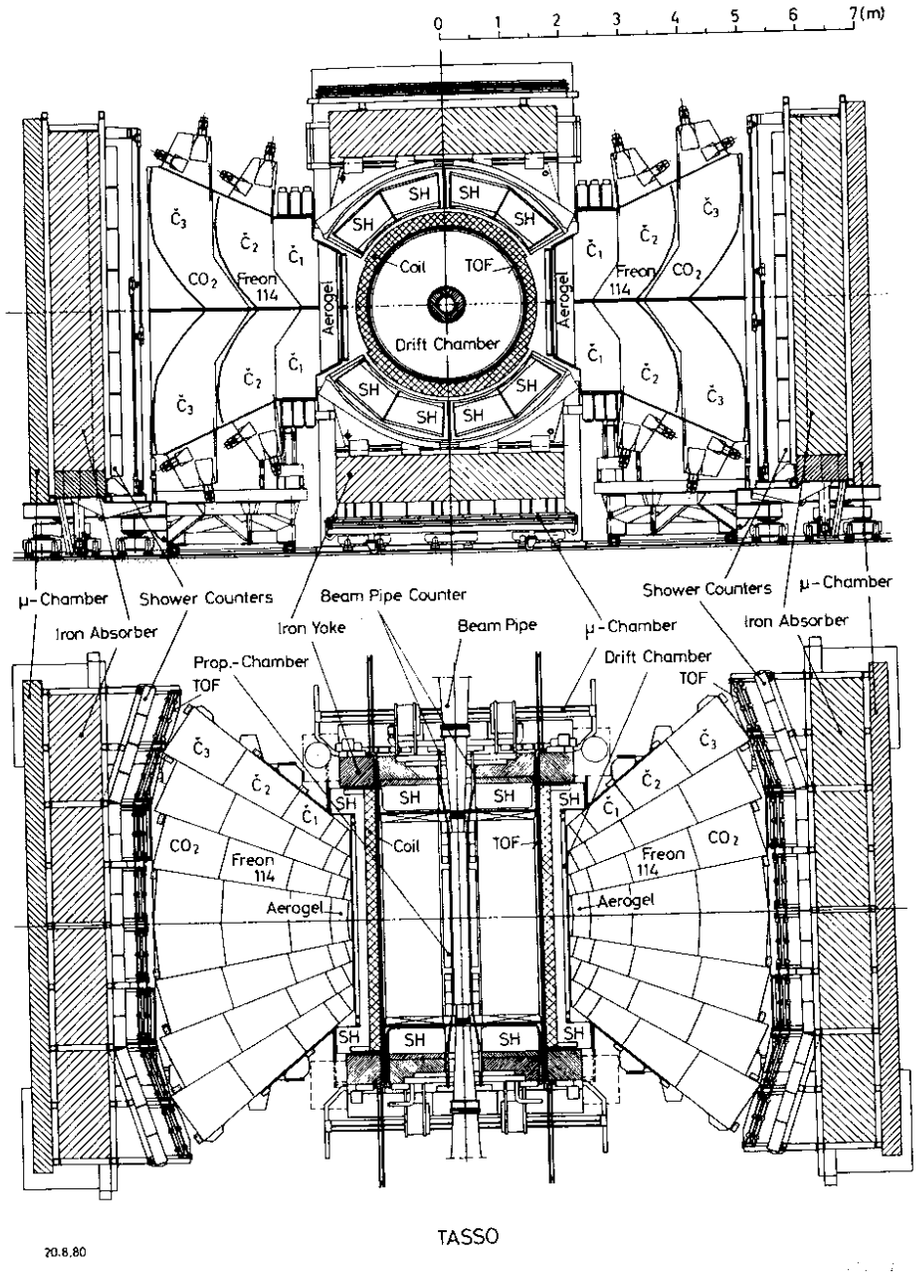

Fig. 1

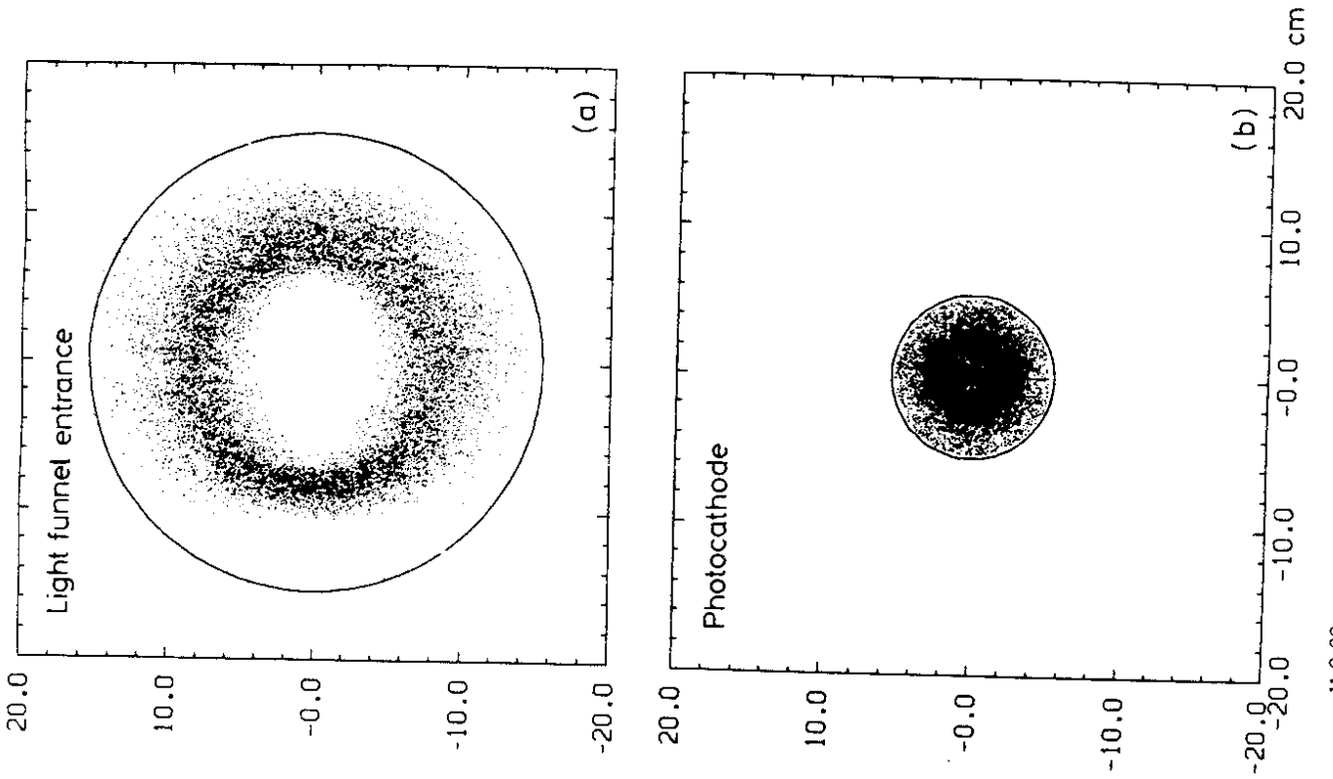
(a)
Light funnel entrance
20.0
10.0
-0.0
-10.0
-20.0
(b)
Photocathode
20.0 cm
10.0
-0.0
-10.0
-20.0
31628
11.9.80

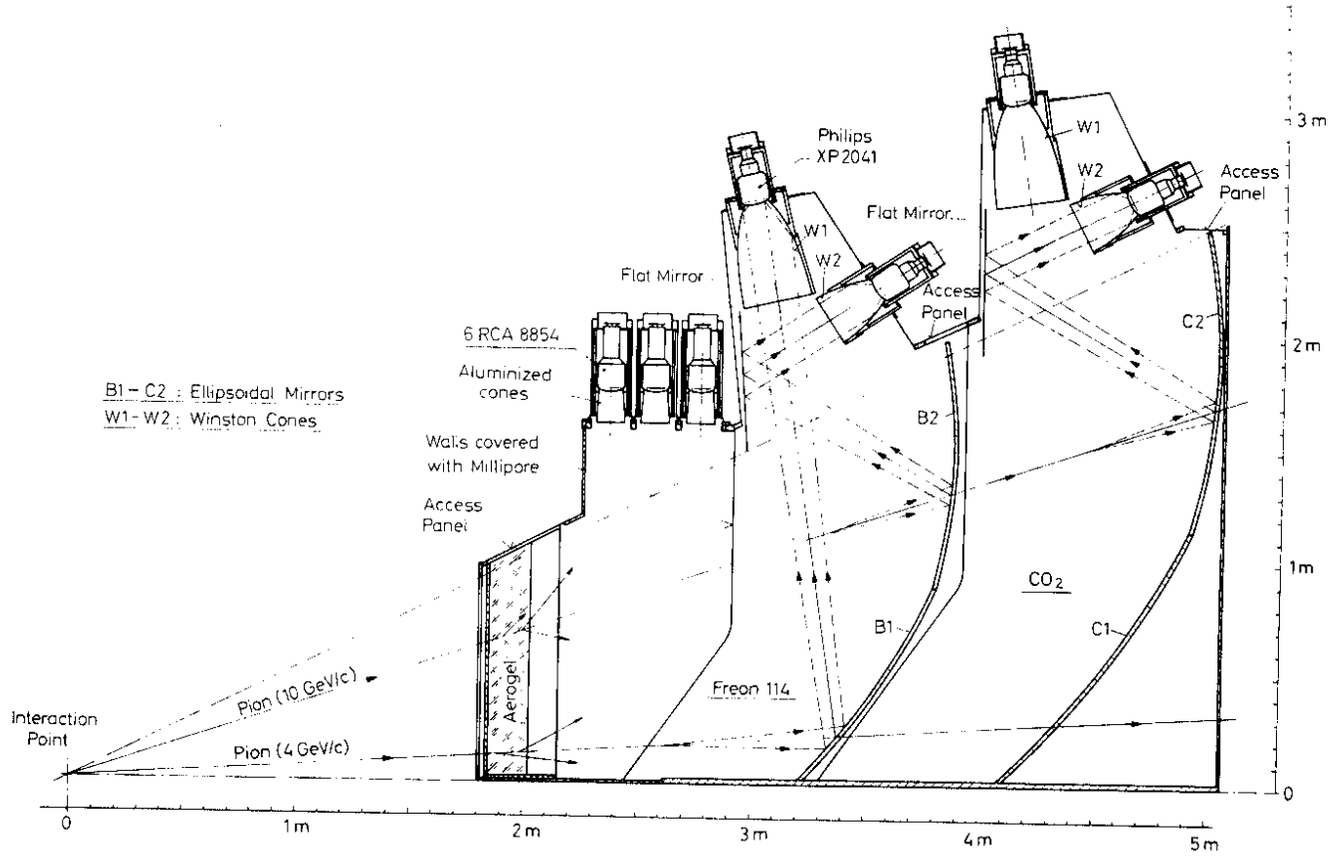
B1 – C2 : Ellipsoidal Mirrors
W1 – W2 : Winston Cones
6 RCA 8854
Aluminized cones
Walls covered with Millipore
Access Panel
Flat Mirror
Philips XP2041
W1
W2
Flat Mirror
Access Panel
W1
W2
Access Panel
C2
B2
CO2
B1
C1
Freon 114
Aerogel
Interaction Point
Pion (10 GeV/c)
Pion (4 GeV/c)
0
1m
2m
3m
4m
5m
3m
2m
1m
0

Fig. 2

30562

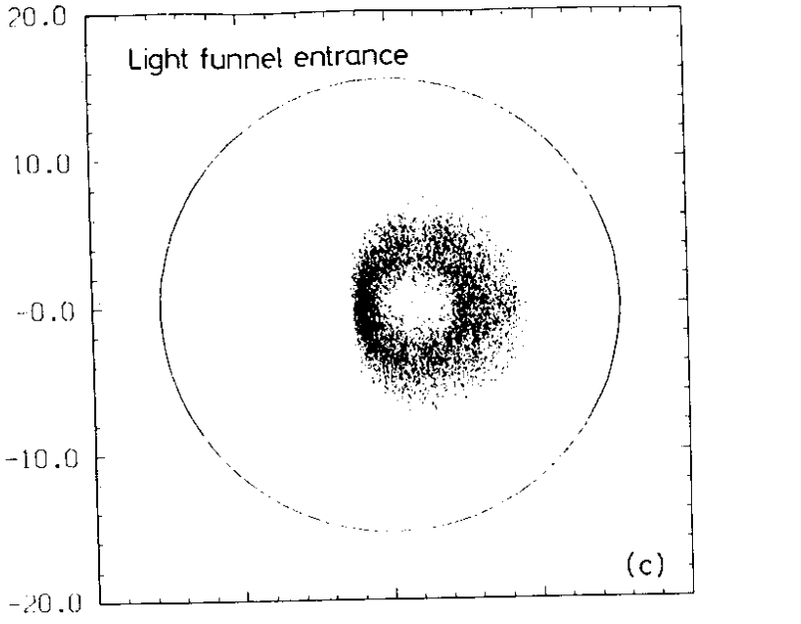

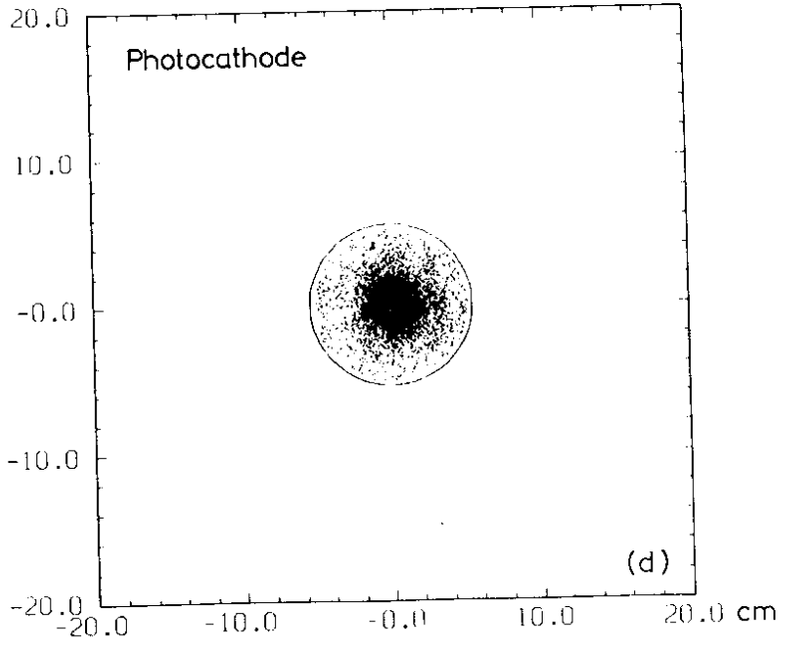

11.9.80

31629

Fig. 3c,d

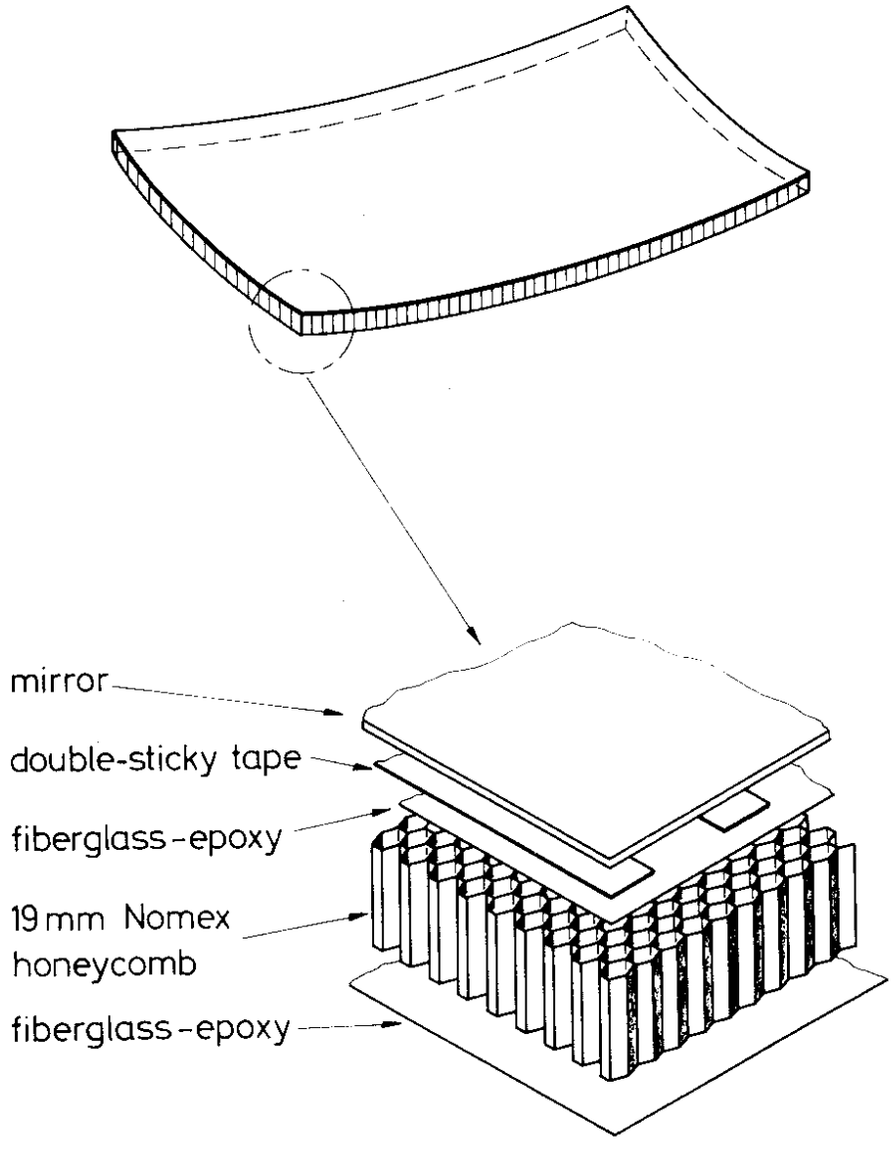

11.9.80

31627

Fig. 4

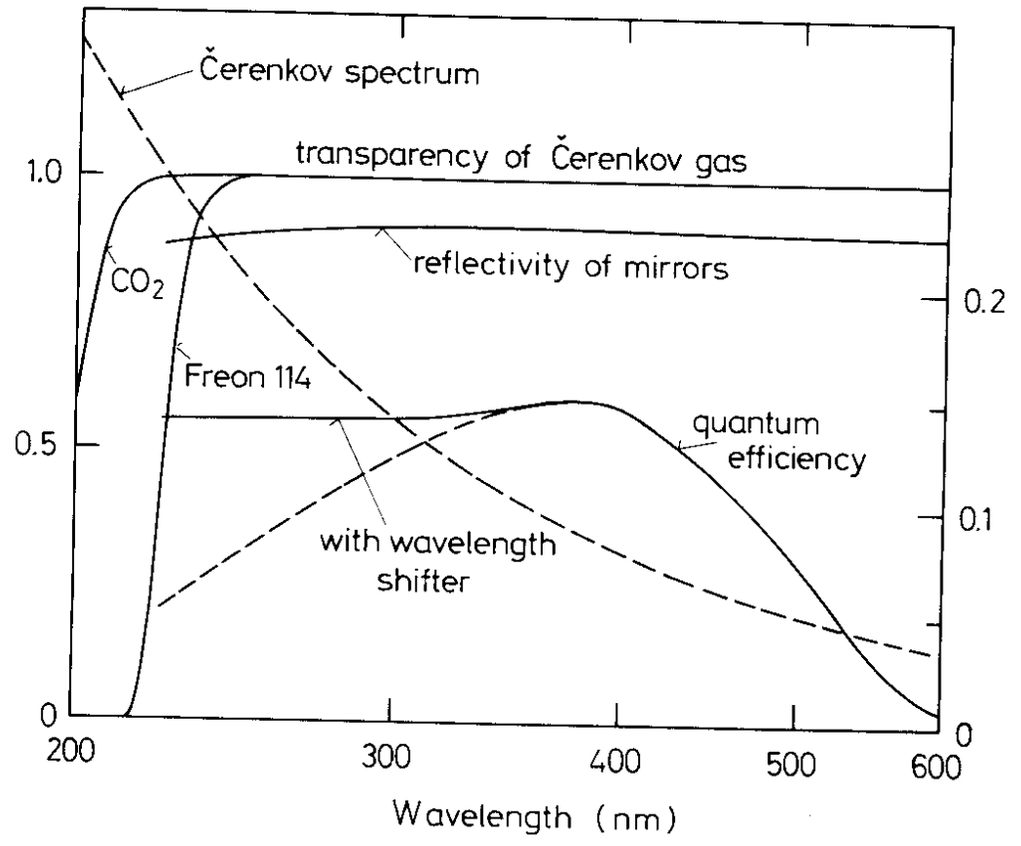
Čerenkov spectrum
transparency of Čerenkov gas
reflectivity of mirrors
CO_2
Freon 114
quantum efficiency
with wavelength shifter
1.0
0.5
0
0.2
0.1
0
200
300
400
500
600
Wavelength (nm)
11.9.80
31626

Fig. 6

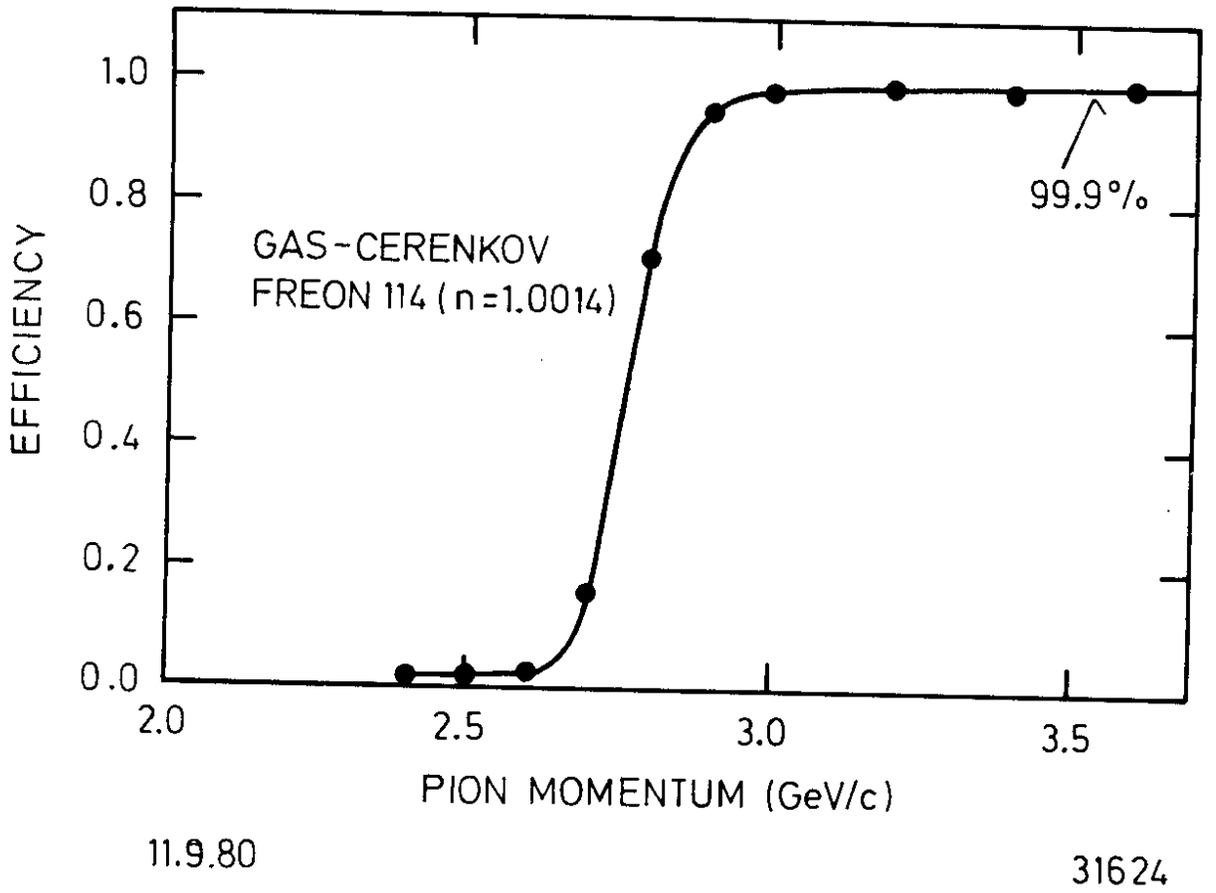
EFFICIENCY
1.0
0.8
0.6
0.4
0.2
0.0
GAS-CERENKOV
FREON 114 (n=1.0014)
99.9%
2.0
2.5
3.0
3.5
PION MOMENTUM (GeV/c)
11.9.80
31624

Fig. 5

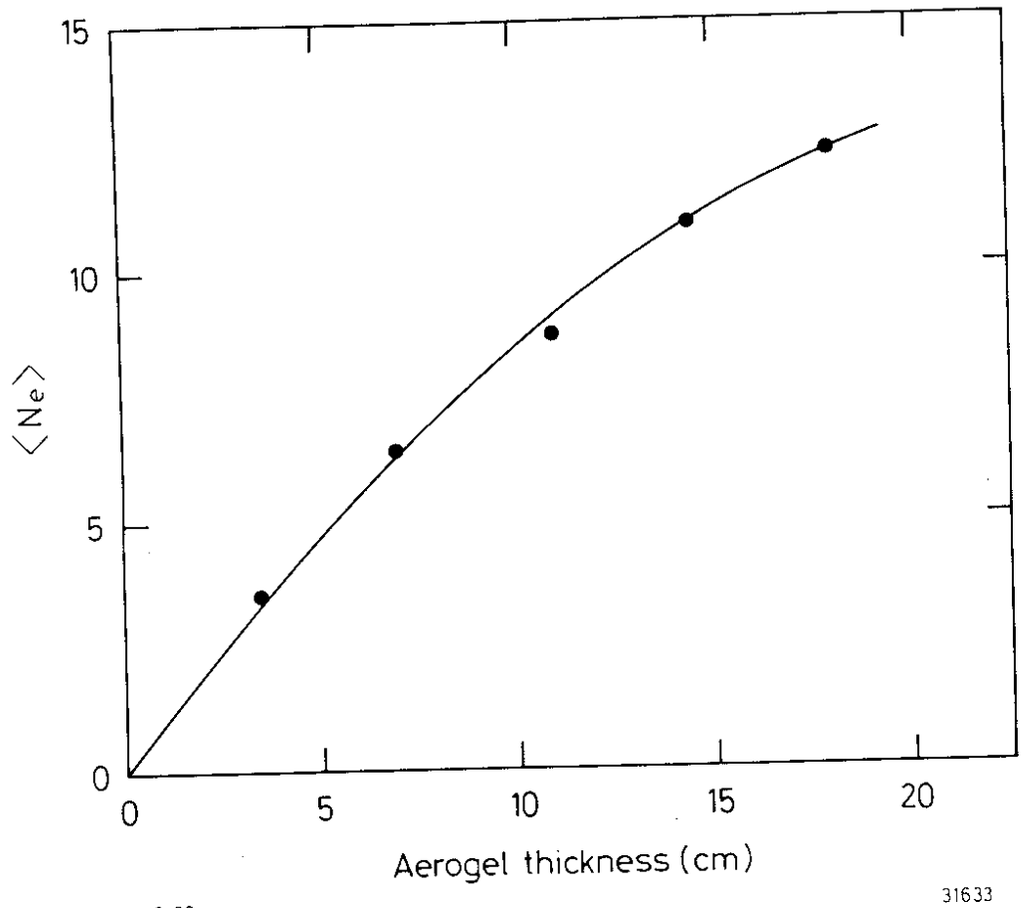

11.9.80

Fig. 7b

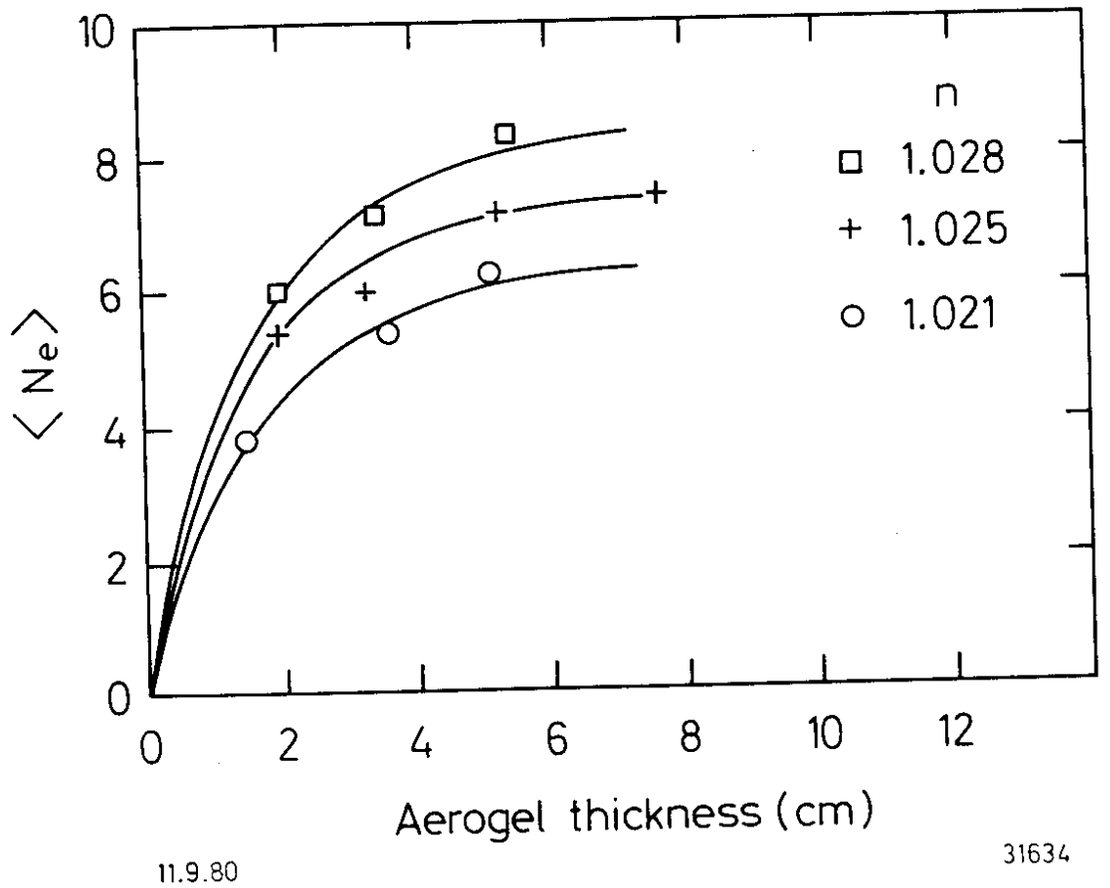

11.9.80

Fig. 7a

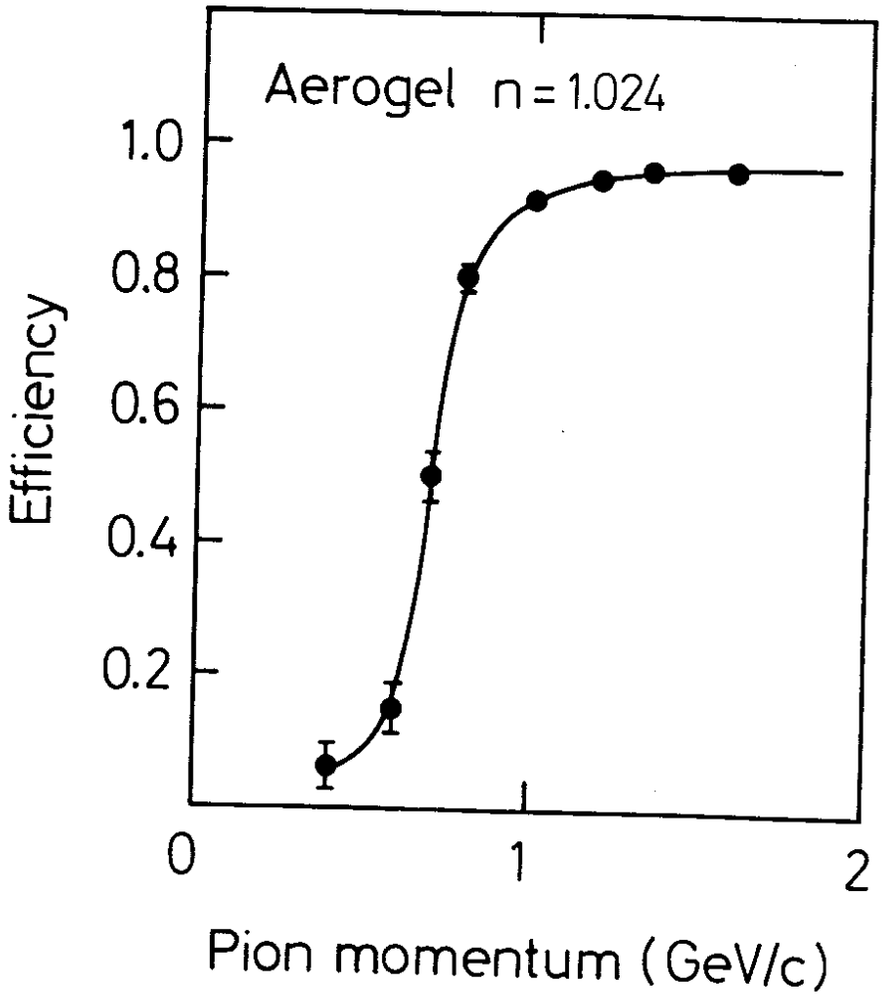

11.9.80

31625

Fig. 8a

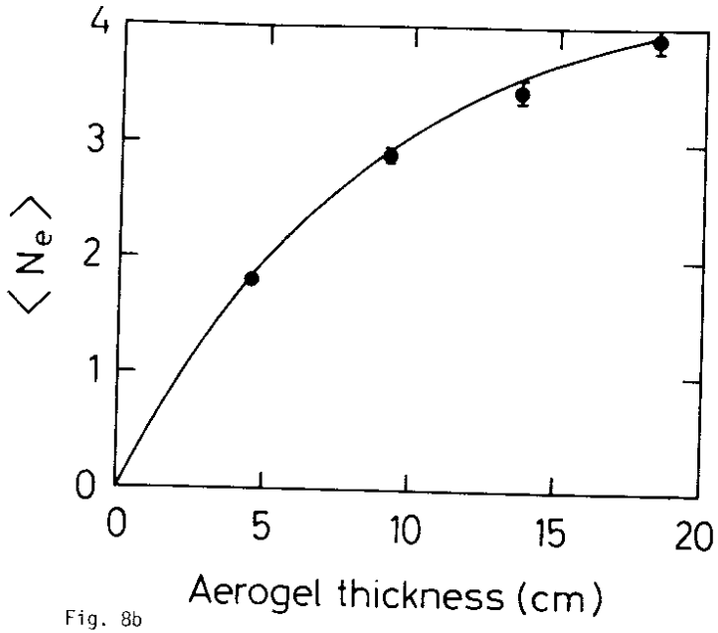

Fig. 8b

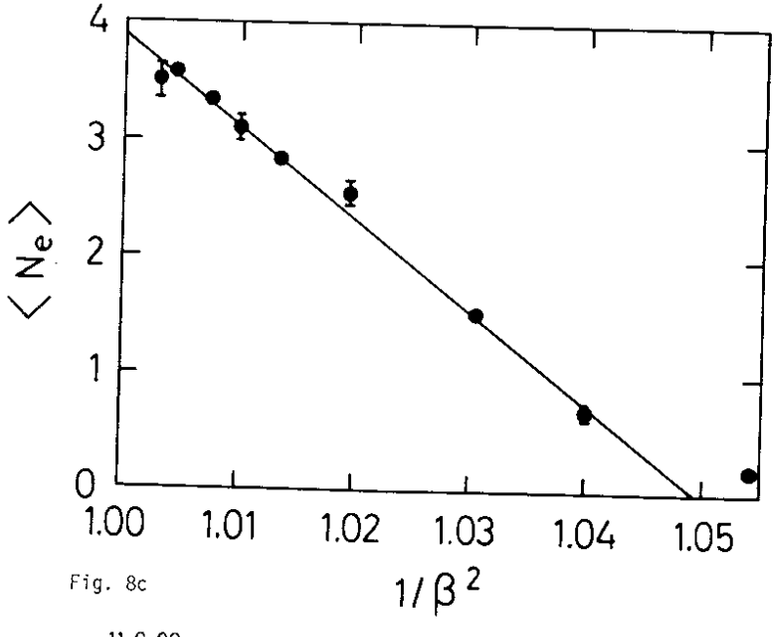

Fig. 8c

11.9.80

31635

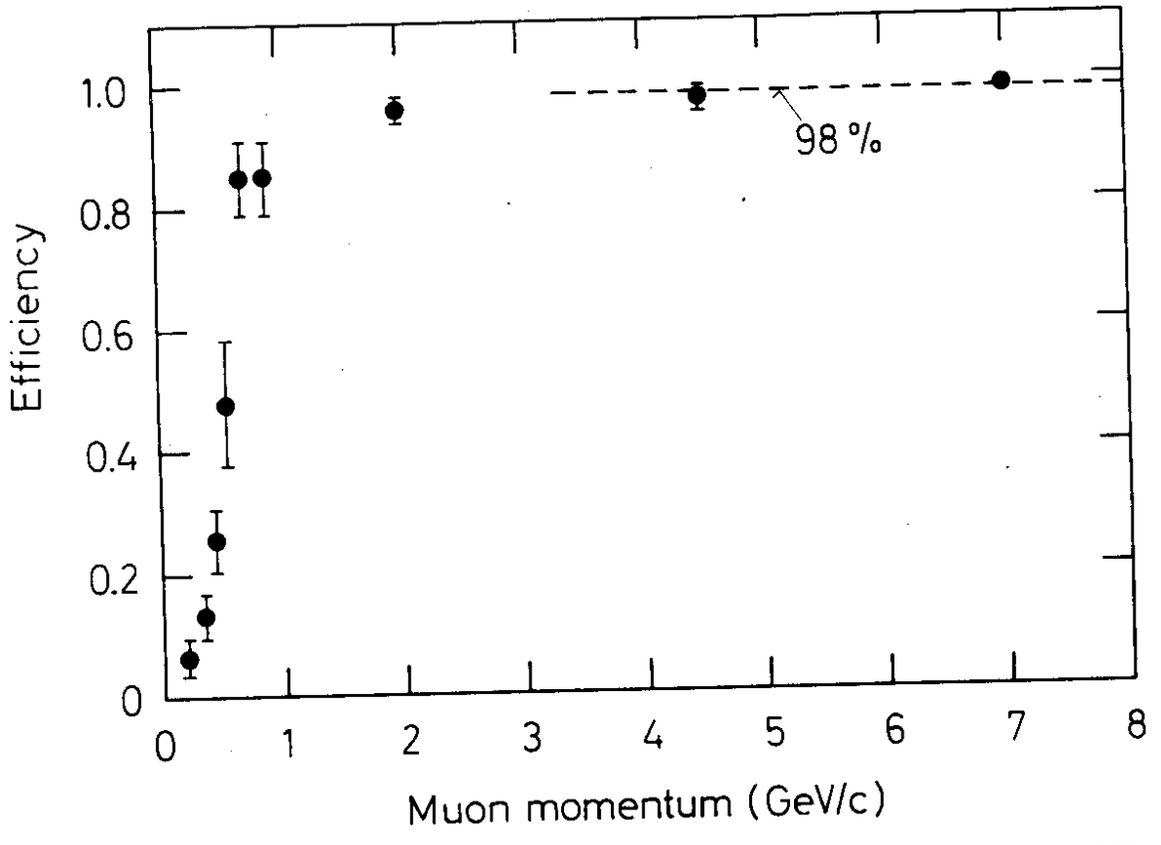

15.9.80

31637

Fig. 9

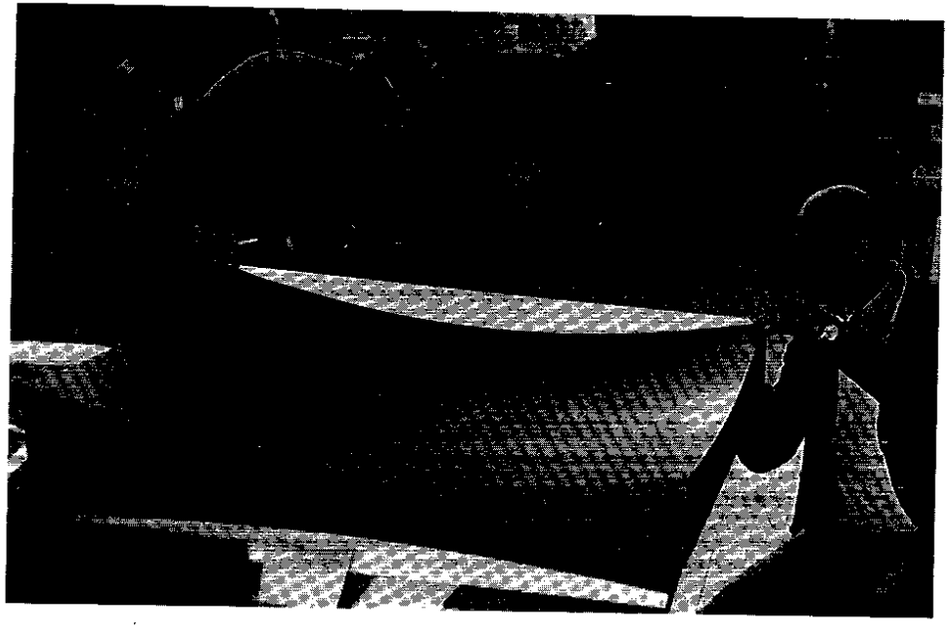

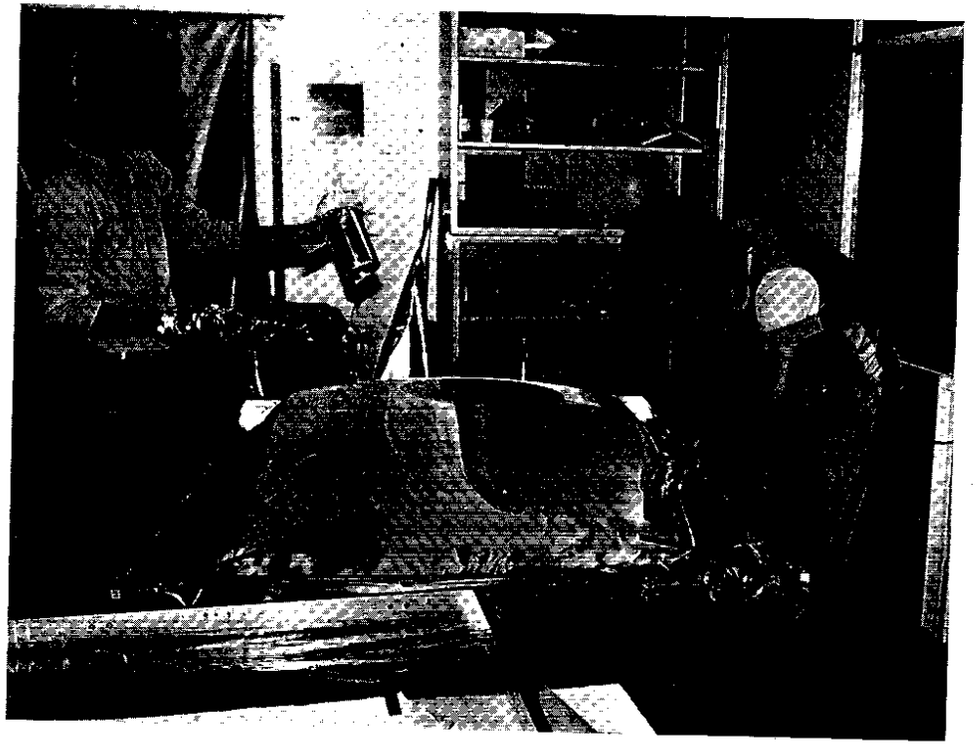

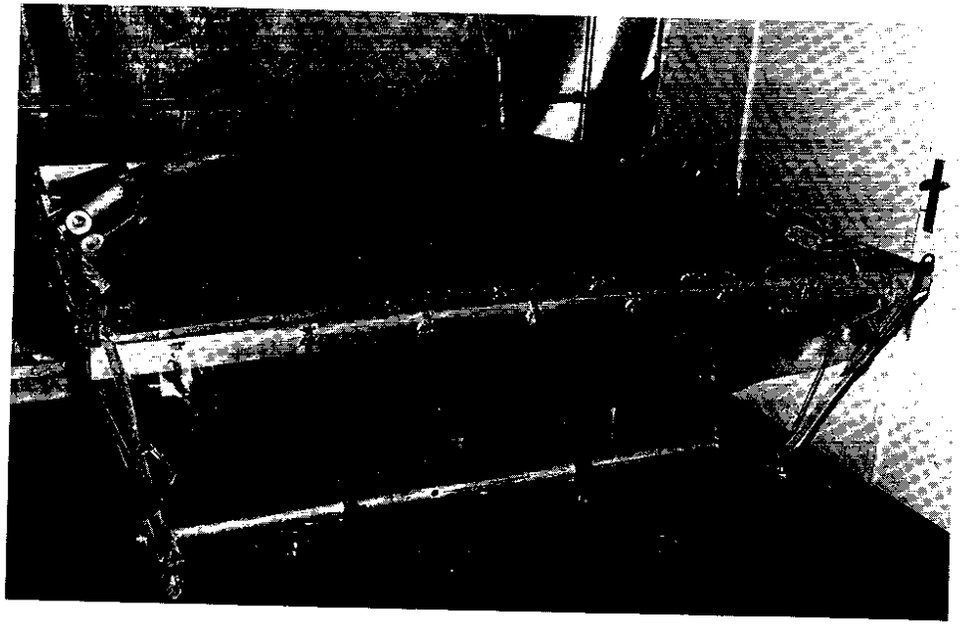

Mirror molds and backings

a) The wooden model of the mold for mirror B2 is checked against the computer-plotted template.

b) The positive mold for mirror B2 is smoothly covered with a stretched 50 µm polyethylene foil and the first layer of fiberglass and epoxy is prepared.

c) Curing of the assembled backing structure. The honeycomb core, sandwiched between two fiberglass-epoxy layers, is pressed firmly against the mold by a 100 µm polyethylene foil which is pulled down by a frame.

The heat-formed plexiglass sheet for mirror B2. The rim of the mold is still visible. It has to be removed with a bandsaw.

Installation of a completed mirror. The plexiglass sheet is first cut to its accurate shape, then aluminized on the front surface and finally glued onto the backing.

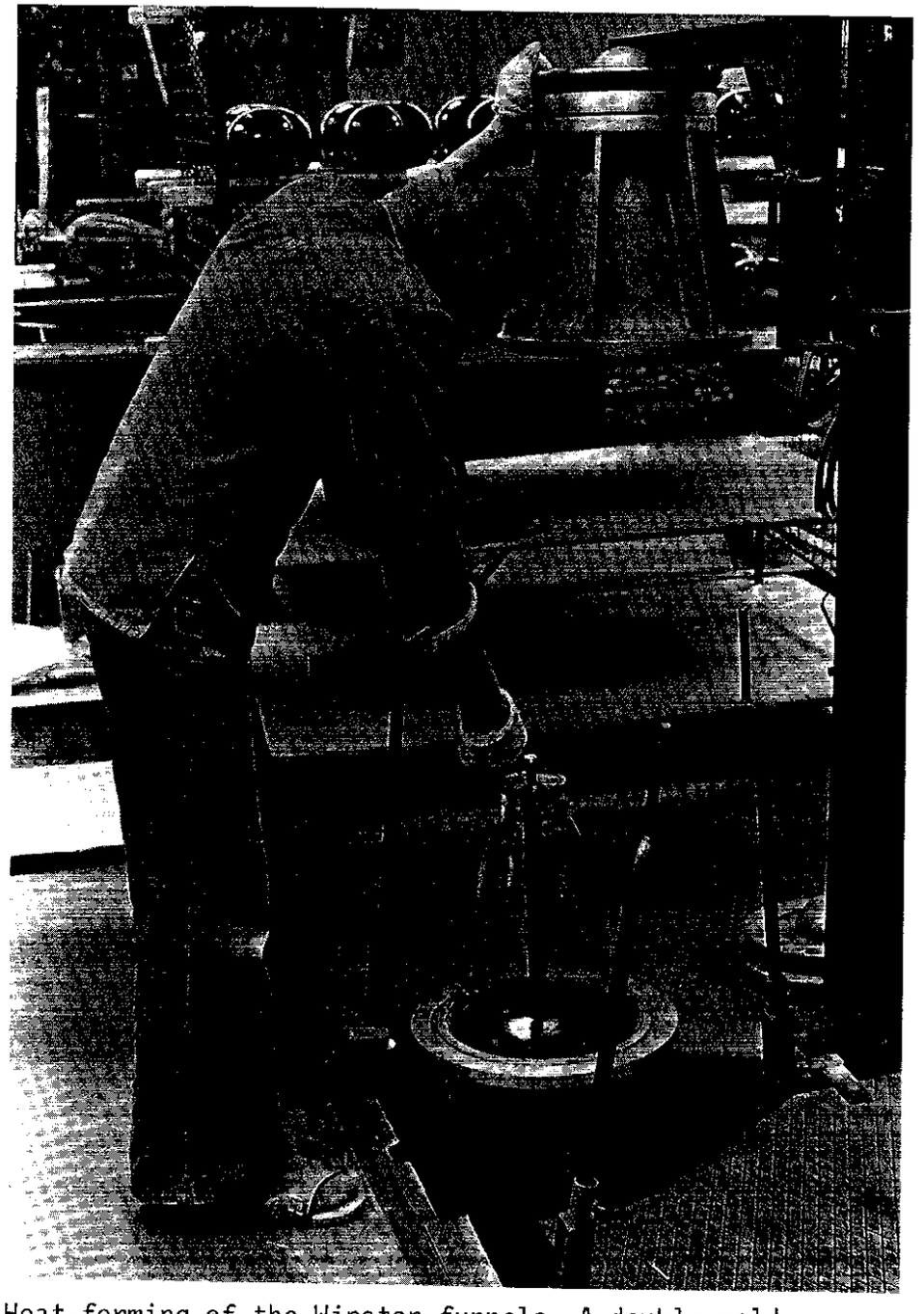

Heat-forming of the Winston funnels. A double mold is used allowing the production of a small and a large funnel in the same step.

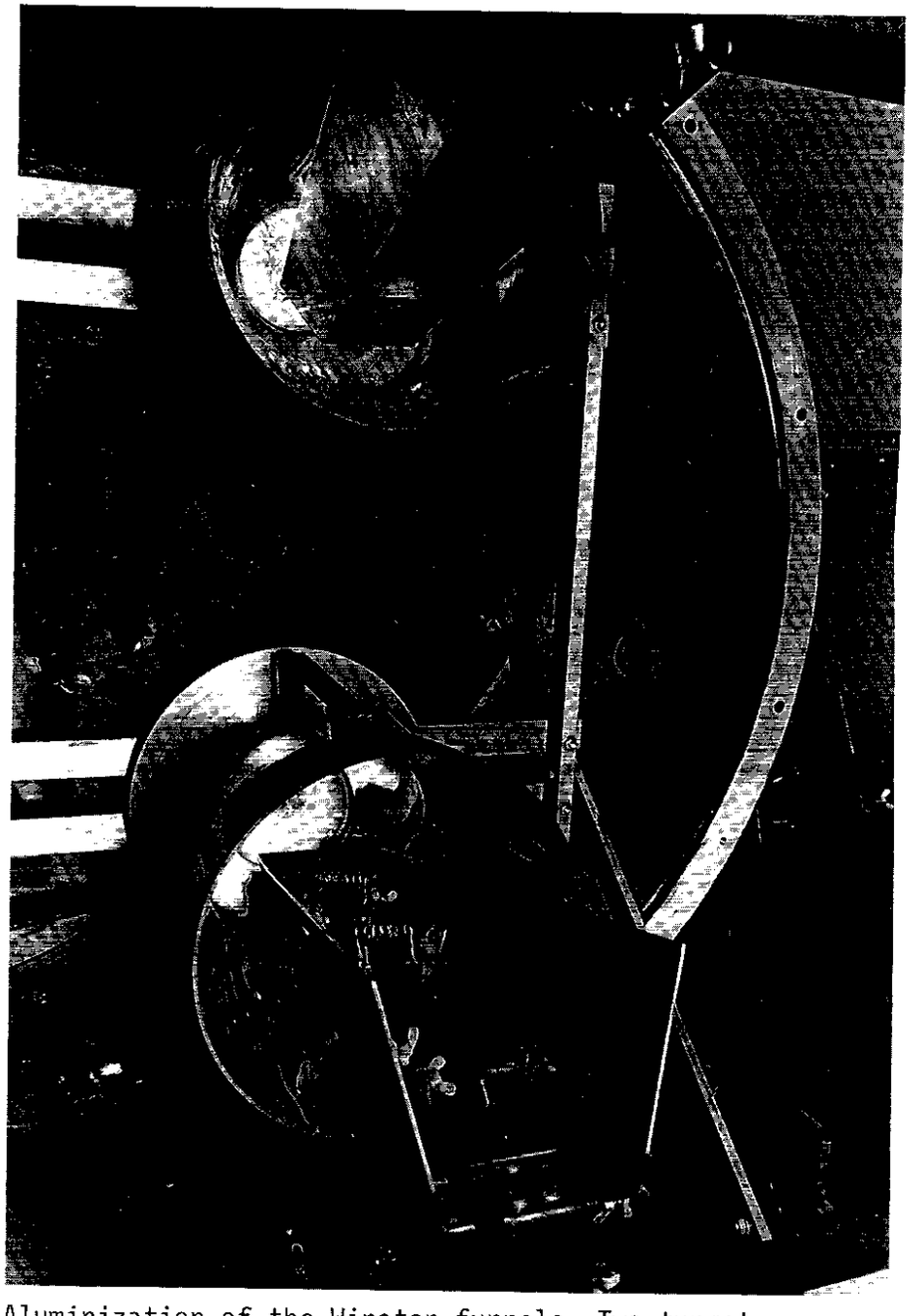

Aluminization of the Winston funnels. Two tungsten coils are used to evaporate the aluminum. The funnels are rotated during evaporation.

The vacuum vessel used to aluminize the mirrors and the Winston funnels.

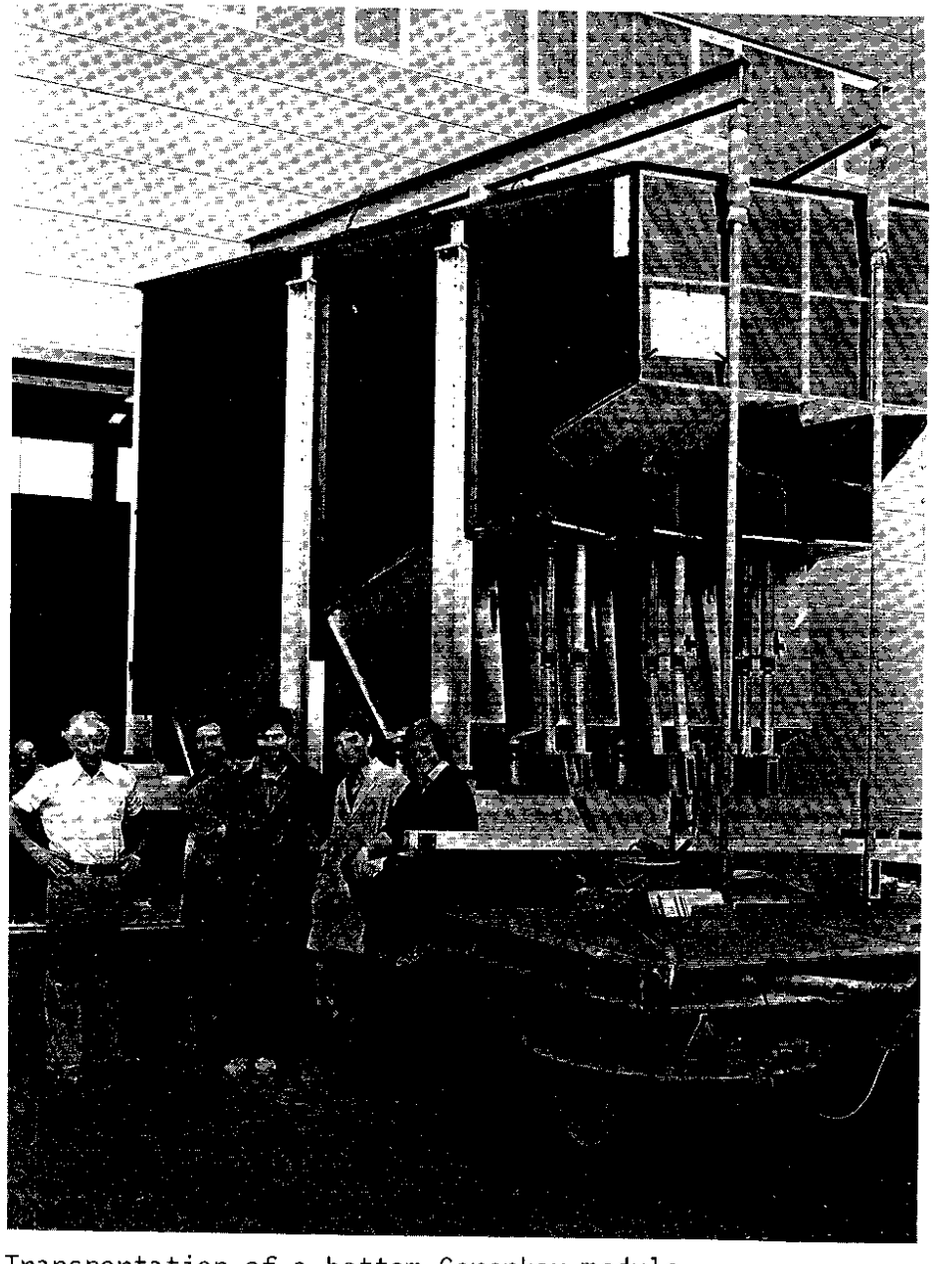

Transportation of a bottom Cerenkov module, consisting of 4 cells of Aerogel, Freon and CO_2 counters.

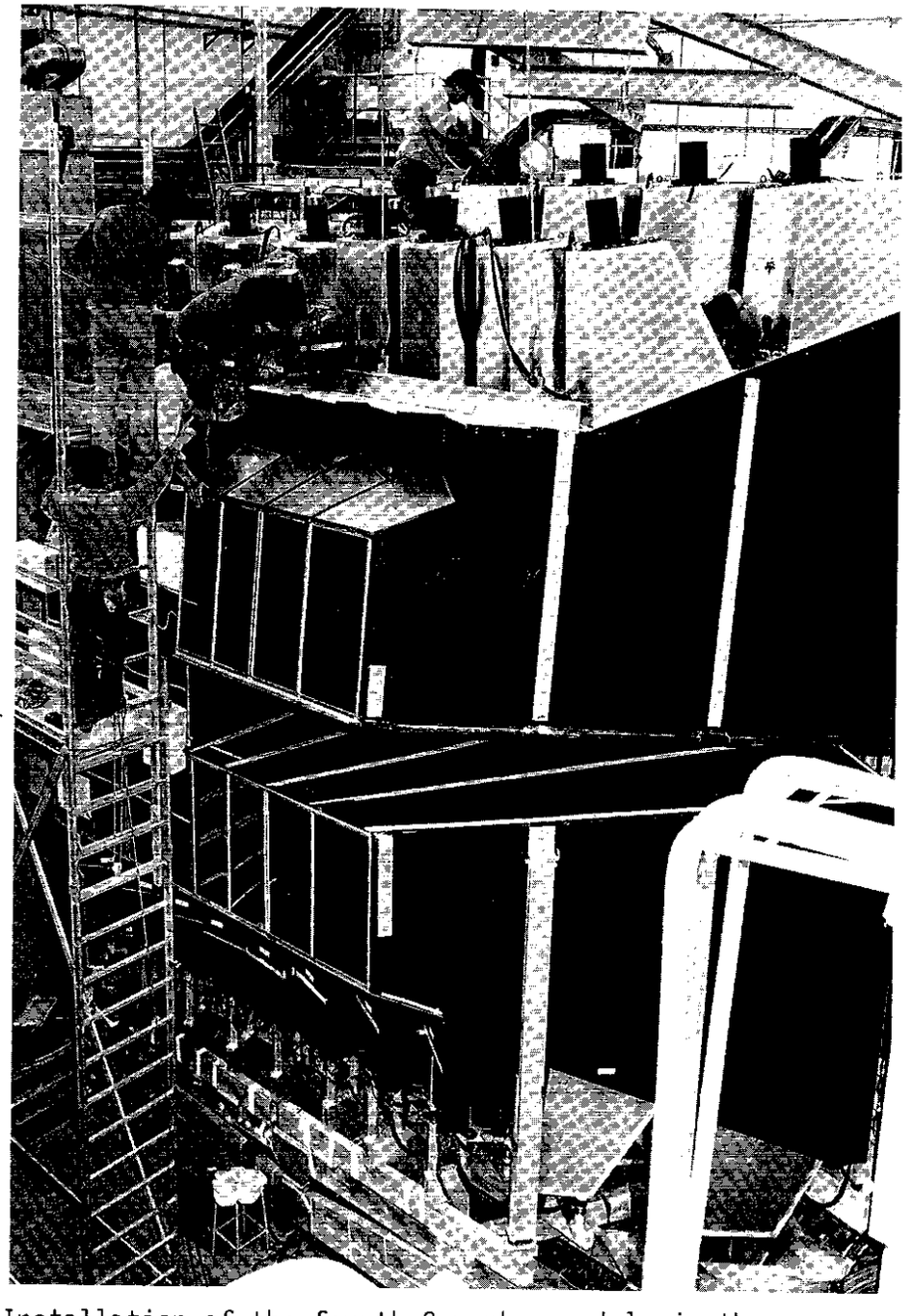

Installation of the fourth Cerenkov module in the TASSO north hadron arm.

A six layer stack of Aerogel. Each Aerogel piece has a size of 17 x 17 x 2.3 cm^3.